^{27}Al NMR/MRI Studies of the Transport of Granular Al$_2$O$_3$

Igor V. Koptyug,[1] *Anna A. Lysova,*[1,2] *Alexey V. Khomichev*[1]*, Renad Z. Sagdeev*[1]

[1] International Tomography Center SB RAS, Novosibirsk, Russia
[2] Boreskov Institute of Catalysis SB RAS, Novosibirsk, Russia

Corresponding author: Igor V. Koptyug, International Tomography Center SB RAS, 3A Istitutskaya St., Novosibirsk 630090, Russia, E-Mail: koptyug@tomo.nsc.ru

Abstract

The NMR/MRI techniques are applicable to the studies of motion of granular solids, providing information on the velocities, effective diffusivities and correlation times of the moving particles. The studies of transport of granular solids reported to-date are based on the detection of the ^{1}H NMR signal of the liquid phase of liquid-containing solid materials. Yet, the solid phase of many granular solids contains magnetic nuclei, providing in principle an opportunity to study motion of such solids by directly detecting the NMR signal of the solid phase. In this paper, we demonstrate that this can be performed with the use of conventional echo pulse sequences in combination with the conventional motion encoding schemes. The detection of the ^{27}Al NMR signal of the Al$_2$O$_3$ powder was used to obtain velocity maps of the powder packed in a spinning cylinder, and to measure the velocity distribution (average propagator) for the gravity driven transport of the same powder in a vertical pipe.

Keywords

NMR imaging, average propagator, granular solid, transport, ^{27}Al NMR

1. Introduction

The NMR/MRI techniques are widely employed to study various types of transport of liquids and gases, including diffusion and quasi-diffusion (dispersion, capillary diffusion, etc.). At the same time, there are various situations of practical and scientific importance where transport of granular solids is diffusion-like. Therefore, both the mathematical formalism and the experimental techniques developed for studying diffusion of liquids and gases can be applicable. Indeed, NMR/MRI techniques have been applied to study transport behavior of granular solids, and such studies have been thoroughly reviewed [1-4].

In particular, granular beds fluidized by means of a flowing gas have numerous applications in industry and include dryers, combustors, and fluidized bed catalytic reactors. Both k-space (MRI) and q-space (PFG NMR, average propagator) techniques were used to evaluate transport properties of solid particles in the fluidized beds and to extract quantitative

characteristics of this transport including effective axial and transverse diffusion/dispersion coefficients [5-7]. More complex experimental schemes can be implemented to distinguish relative contributions of coherent (differences in particles' velocities) and incoherent (modulation of each particle's velocity by random collisions) motion to dispersion, and to estimate correlation times of particles' motion [8]. Similar strategies can be employed to study the transport of gas used for bed fluidization, if appropriate NMR signal enhancement techniques such as hyperpolarization of [129]Xe are employed [9,10].

Fluidization of granular material can be also achieved by vibrations of a container. Spin-tagging technique [11-14], for instance, was used to study such transport, with the distortion of tags reflecting flow of solid particles, and the blurriness of the stripes characterizing particles' diffusion. The average propagator measurements of particles' displacements in vibrofluidized beds were performed either without [15] or with spatial resolution [16,17]. In the latter case, a crossover from the ballistic to the diffusive regime was observed for an increasing displacement interval. Transport of granular materials in rotating drums is also used in many technological processes such as granulation, mixing, milling, drying, calcination, coating, etc. Several NMR/MRI studies address the flow of granular material in horizontal rotating drums [18-25]. Maps of apparent particle diffusivities along all three spatial directions were obtained [19]. More sophisticated measurements of the time-dependent apparent diffusivities can be utilized to separate correlated and random motion, which allows one to obtain spatial maps of the correlation time and of the long time limit diffusivity values [20]. The PFG NMR technique was also used to detect average propagators in the course of the gravity driven filtration of fine alumina particles in a granular bed [26]. The results have revealed the bimodal character of particles' velocities distribution, and demonstrated that the average filtration velocity was highest at an intermediate mass flow rate before the onset of the bed flooding.

The studies mentioned above demonstrate once again the usefulness of the NMR/MRI techniques to study the structure and dynamics of bulk opaque materials and their advantages as compared to other instrumental techniques. Yet, all the studies of solids transport performed so far required the use of liquid-containing solids and were based on the detection of the strong and slowly relaxing ^{1}H NMR signal of the liquid phase. To this end, materials with high content of oil, water or other proton-containing liquids were used as model granular materials (poppy and mustard seeds, liquid-containing pharmaceutical pills, liquid-saturated porous grains), making the arsenal of NMR/MRI techniques developed for liquids and gases applicable to such studies. At the same time, it could be advantageous to study mass transport of solid materials by directly detecting the NMR signal of the moving solid. Indeed, many technologically important solid materials (e.g., catalysts, ceramics, glasses, minerals, etc.) contain magnetic nuclei and therefore can be potentially studied with the NMR/MRI techniques.

The NMR/MRI studies of solids, however, are hampered to a significant extent due to the fact that low molecular mobility and anisotropic interactions lead to very broad NMR resonances. This is especially true for rigid solids and for quadrupolar ($I > 1/2$) nuclei for which quadrupolar broadening effects can easily lead to line widths in excess of 1 MHz. As a result, MRI of rigid solids has not by now become a wide-spread routine application, mostly, it appears, because such experiments are usually associated with the utilization of the powerful arsenal of specialized solid state NMR hardware and techniques and large magnetic field gradients [27]. At the same time, examples of MRI applications to the studies of rigid solids containing quadrupolar nuclei have been published in the literature. In particular, it has been demonstrated that the central transition of quadrupolar [27]Al nucleus ($I = 5/2$) in alumina and ceramics can be refocused using conventional spin-echo sequences, thereby making it possible to perform multidimensional [27]Al imaging of solid materials [28-30]. We have

demonstrated recently that in fact a number of rigid solid materials containing various quadrupolar nuclei ([7]Li, [11]B, [23]Na, [27]Al, [29]Si, ^{31}P, [51]V) can be imaged using the conventional two-pulse spin echo sequence on a commercial liquid phase NMR microimaging instrument [31-35]. The fact that solid materials can be imaged without a need to resort to the arsenal of solid state NMR/MRI can significantly accelerate the progress in the development of such applications. In this work, we demonstrate that these studies can be extended to MRI and PFG NMR of the transport of rigid solids with the direct detection of the NMR signal of the solid phase.

2. Methods and Materials

Alumuina powder (32% γ-Al$_2$O$_3$, 68% χ-Al$_2$O$_3$) with the particle sizes in the range 0.08-0.2 mm was used in all experiments. The pores of the alumina particles contained 8% by weight of Vaseline oil since this powder was used earlier in the average propagator measurements with ^{1}H NMR signal detection [26]. To mechanically spin a Teflon cell packed with alumina powder inside the NMR probe of the vertical-bore NMR system, an aluminum rod was attached to the bottom of the cell. It served as a spinning shaft, with its lower end connected to an electrical motor via a rubber band so that the motor could be placed outside the stray field region of the superconducting NMR magnet. To study the gravity driven flow of alumina powder, a copper funnel was positioned above the bore of the superconducting magnet. A rubber hose with 11 mm inside diameter attached to the bottom of the funnel was passing all the way through the magnet bore and the rf probe, ending in an aluminum container located below the magnet. In the beginning of an experiment, the funnel was filled with the alumina powder, which freely flowed downward in the rubber hose and accumulated in the aluminum container. During the measurements, the granular material was periodically manually transferred from the collecting container to the feeding funnel to ensure an uninterrupted flow of alumina powder during each experiment. Further details can be found elsewhere [26].

All ^{27}Al NMR/MRI experiments were performed at 78.2 MHz with a 7 T Bruker Avance DRX-300 wide-bore spectrometer equipped with imaging accessories and a home-built probe with a 25 mm i.d. saddle-shape rf coil. All imaging experiments used the two-pulse spin echo sequence (α-τ-2α-τ-echo), while velocity mapping and average propagator measurements were performed using the three-pulse stimulated echo sequence (α-τ-α-T-α-τ-echo). The nominal flip angle was set to $\alpha = 30°$ (=$90°/(I + 1/2)$ [29,36,37]). It was calibrated using an aqueous solution of AlCl$_3$. 2D images in the transverse (XY) plane were acquired without slice selection. From 16 to 64 complex data points were detected per echo signal, with the echo time of 600-800 µs. In the velocity imaging experiments, the images detected were 16×16 pixels with (1.5 mm) × (1.5 mm) spatial resolution, acquired with NA=64 averages and the repetition time of TR=0.15 s, corresponding to the total acquisition time of 43 min per image. Pure phase encoding was used to obtain spatial resolution in two dimensions (no frequency encoding). Along with the gradients for spatial encoding, a bipolar pair of gradients was added to achieve velocity encoding. Each gradient of the bipolar pair was δ=200 µs long and g=9.8 G/cm in amplitude, and their centers were separated by Δ=1.8 ms. For each of the two velocity components in the imaging plane, two experiments were performed: one with a static sample and another with a sample spinning at 22 rps. The velocity maps were then calculated by evaluating the signal phase difference for each pixel of these two images. For the average propagator measurements, we used the stimulated echo pulse sequence with the motion encoding bipolar gradient pair with δ=300 µs, Δ=5.2 ms and g=98 G/cm incremented from −g to g in 32 steps. The filter width was set to 20 kHz in all experiments to improve signal-to-noise ratio of the detected signal.

3. Results and discussion

The results of the velocity mapping experiments performed for the spinning cell packed with alumina powder are presented in Fig. 1. The maps obtained are in good agreement with the expected velocity distributions, both qualitatively and quantitatively. Indeed, the x component of the linear velocity (V_X) in the plane transverse to the axis of rotation is expected to be constant along the x coordinate and to be proportional to the y coordinate, in a qualitative agreement with the map obtained. A similar behavior is observed for V_Y. Furthermore, the velocity components are in a good quantitative agreement with the linear velocities calculated from the known sample spinning rate and the sample diameter. The experimental maps appear slightly rotated, which is brought about by the fact that during the pulse sequence, the spatially encoding gradient is applied simultaneously with the first gradient pulse of the bipolar pair used for motion encoding, whereas the second gradient pulse of the bipolar pair is applied ca. 1.8 ms later. This implies that spatial encoding and motion encoding are not performed at the same instance in time, leading to an apparent rotation of the detected velocity maps. The angle of apparent rotation is half the value of the actual rotation angle of the sample between the two pulses of the bipolar gradient pair, and the direction of the apparent rotation is opposite to the direction of the actual rotation of the sample.
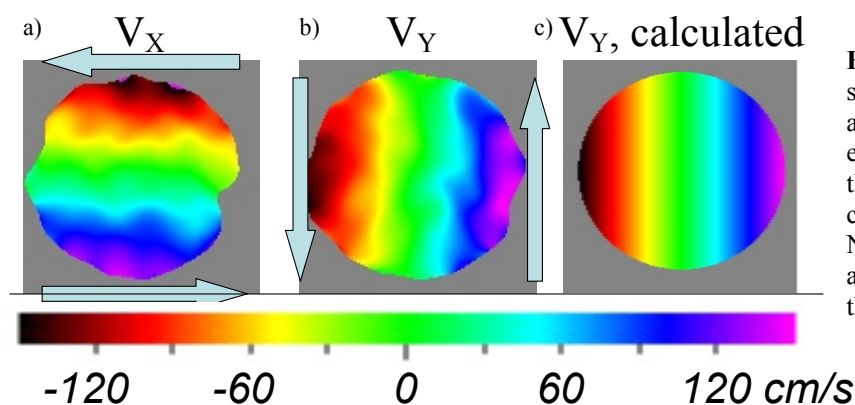

Fig. 1: Velocity maps for the spinning cylinder packed with alumina powder. The experimentally measured maps for the V_X (a) and V_Y (b) velocity components detected using the ^{27}Al NMR signal of alumina are shown along with the calculated map for the V_Y component of velocity.

Next, to check the applicability of the PFG NMR average propagator measurements to the studies of solid particles' transport by directly detecting the NMR signal of the solid phase, we have performed a series of experiments with the alumina powder freely flowing (falling) in a vertical rubber hose under the action of gravity. The results of one such measurement are presented in Figs 2 and 3. In Fig. 2, the dependence of the echo signal on the amplitude of the gradients of the motion-sensitizing bipolar pair is presented. It is clear from the figure that a pronounced variation of the echo signal phase is observed as the amplitude of the gradients is changed in a step-wise manner. It is also obvious that the echo decay for the largest absolute values of the gradients is not very pronounced. This is an indication that the velocity distribution for the ensemble of the falling particles is quite narrow, leading to an insignificant dephasing of the transverse magnetization and little signal decay as the gradient is varied. The average propagator obtained after Fourier transformation of the echo signal dependence on the gradient amplitude of Fig. 2 is shown in Fig. 3. As can be seen, the alumina particles pass the detection region with a velocity of ca. 10 cm/s. The fact that there is little decay of the echo signal at large gradient amplitudes in Fig. 2 leads to the appearance of Gibbs ringing in the propagator presented in Fig. 3. Furthermore, a factor of four zero-filling of the data performed before Fourier transformation broadens the propagator, therefore its width is no longer a reliable measure of the width of the velocity distribution. Indeed, as suggested by Fig. 2, the distribution of velocities is very narrow, and its accurate evaluation would require a

larger range of q values to be sampled, something which is not easily achievable at the moment.

To the best of our knowledge, neither MRI velocimetry nor average propagator measurements with the direct detection of the NMR signal of the solid phase have been
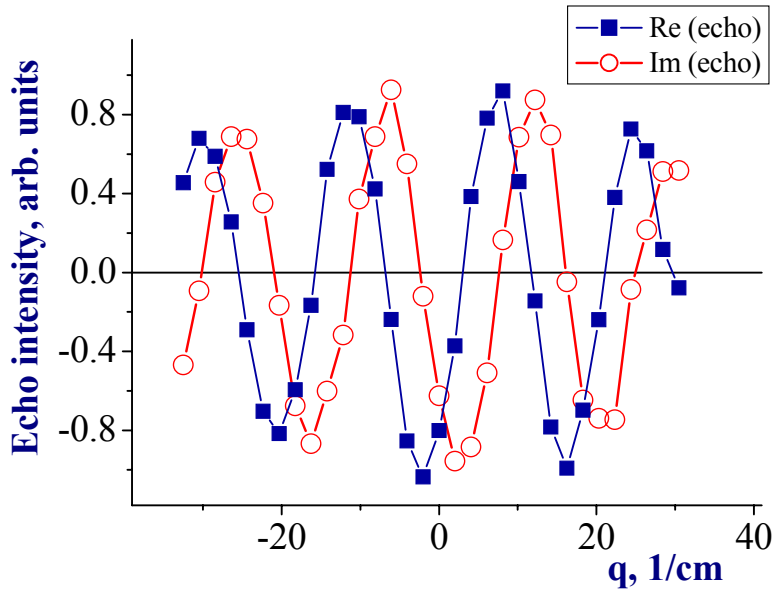

Fig. 2: Modulation of the ^{27}Al stimulated echo signal intensity as a function of gradient amplitude ($q=\gamma\delta g/2\pi$, $\delta=0.3$ ms, $\Delta=5.53$ ms) detected in the course of the gravity driven flow of alumina powder in a vertical pipe. Both the real (■) and the imaginary ( ) components of the complex echo signal are shown in the figure.

reported earlier. The results presented above demonstrate that conventional spin or stimulated echo techniques and motion encoding schemes are applicable to the direct detection of motion of solid samples and materials. It is clear that multinuclear NMR/MRI techniques can be extended to the studies of other motion and transport processes of solid samples possessing suitable magnetic nuclei. In particular, it should be possible to extend these studies to cover granular material transport in horizontal rotating cylinders as well as in gas-fluidized or vibrofluidized beds mentioned in the Introduction. The usefulness of these approaches will depend on the sensitivity achievable in the solids NMR/MRI experiments, therefore we are currently considering various ways of improving sensitivity in such experiments [34].
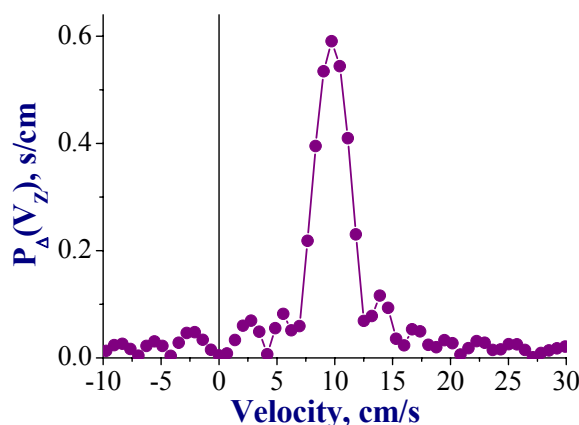

Fig. 3: The average propagator obtained for the gravity driven flow of solid alumina particles by a four-fold zero-filling of the data set of Fig. 2 with a subsequent Fourier transformation.

One of the disadvantages of the motion encoding experiments using nuclei other than ^{1}H is the lower sensitivity of low-gamma nuclei to the magnetic field gradients, since the flow-induced variation of the signal phase is proportional to the magnetogyric ratio of the detected nucleus, and the logarithm of the signal attenuation in a PFG NMR experiment is proportional to the square of the magnetogyric ratio. For instance, for ^{27}Al the resonance frequency (i.e.,

the magnetogyric ratio) is almost a factor of four lower than for protons, leading to a lower sensitivity to the motion encoding gradients. Furthermore, the transverse relaxation time T_2 is short [31], limiting the maximum separation of the gradient pulses in the bipolar pair and thus further reducing the sensitivity to motion. Fortunately, for the ^{27}Al NMR signal of alumina, the spin-lattice relaxation time T_1 is much longer than T_2 [31]. Therefore, the stimulated echo sequence is preferable for such experiments. For instance, in our PFG NMR experiments with alumina, the separation of the gradient pulses in the bipolar pair of a few hundred ms could be used, if necessary, with still enough signal for detection.

At the same time, despite the drawbacks mentioned above, the direct detection of the NMR signal of the solid phase in the studies of the transport of solid materials has important advantages, too. In particular, it eliminates the need to use liquid-containing particles. This can provide an opportunity to study transport of granular solids unperturbed by the presence of the liquid phase (for instance, in the case of porous particles impregnated with a liquid). Furthermore, this approach can potentially extend the range of solid materials that can be used in such NMR/MRI studies. We believe that this area of research deserves further attention.

4. Conclusions

In this work, we have demonstrated that the three-pulse stimulated echo pulse sequence in combination with the conventional motion encoding schemes can be used to study transport of solid materials by directly detecting the NMR signal of the solid phase. As an example, we have used the ^{27}Al NMR signal of alumina powder. Velocity mapping was performed for the powder packed in a spinning cylinder, demonstrating the possibility to detect maps of the two velocity components in the plane perpendicular to the axis of rotation. In the case of a gravity driven flow of the alumina powder in a vertical pipe, the PFG NMR experiment was employed to detect the average propagator for the particles' motion. The results demonstrate the feasibility of such experiments, and in particular that the relaxation times of the NMR signal are sufficiently long to detect the echo signal of the quadrupolar ^{27}Al nuclei of solid alumina particles with a reasonable sensitivity and to ensure an adequate motion sensitization despite the lower magnetogyric ratio as compared to protons.

References

[1] E. Fukuishima, in Stapf, S., Han, S. (Eds.), NMR Imaging in Chemical Engineering. Wiley-VCH, Weinheim, 2005, pp. 490-508.
[2] E. Fukushima, Adv. Comp. Sys. 4 (2001) 503-507.
[3] I.V. Koptyug, R.Z. Sagdeev, Russ. Chem. Rev. 71 (2002) 789-835.
[4] M.D. Mantle, A.J. Sederman, Progr. NMR Spectr. 43 (2003) 3-60.
[5] P.S. Fennell, J.F. Davidson, J.S. Dennis, L.F. Gladden, A.N. Hayhurst, M.D. Mantle, C.R. Muller, A.C. Rees, S.A. Scott, A.J. Sederman, Chem. Engng Sci. 60 (2005) 2085-2088.
[6] R. Savelsberg, D.E. Demco, B. Blümich, S. Stapf, Phys. Rev. E 65 (2002) 020301.
[7] S. Stapf, A. Khrapitchev, C. Heine, S. Harms, and B. Blümich, in: Modern Magnetic Resonance, Volume 3: Applications in Materials, Food and Marine Sciences Webb, G.A. (Ed.) Springer, 2006.
[8] S. Harms, S. Stapf, B. Blümich, J. Magn. Reson. 178 (2006) 308-317.
[9] R. Wang, M.S. Rosen, D. Candela, R.W. Mair, R.L. Walsworth, Magn. Reson. Imaging 23 (2005) 203-207.
[10] R. Wang, M.S. Rosen, D. Candela, R.W. Mair, R.L. Walsworth, Chem. Engng Technol. 23 (2005) 203.
[11] E.E. Ehrichs, H.M. Jaeger, G.S. Karczmar, J.B. Knight, V.Yu. Kuperman, S.R. Nagel, Science 267 (1995) 1632-1634.

[12] V.Yu. Kuperman, E.E. Ehrichs, H.M. Jaeger, G.S. Karczmar, Rev. Sci. Instr. 66 (1995) 4350-4355.

[13] V.Yu. Kuperman, Phys. Rev. Lett. 77 (1996) 1178-1181.

[14] J.B. Knight, E.E. Ehrichs, V.Yu. Kuperman, J.K. Flint, H.M. Jaeger, S.R. Nagel, Phys. Rev. E 54 (1996) 5726-5738.

[15] D. Candela, A. Ding, X. Yang, Physica B 279 (2000) 120-124.

[16] X.Y. Yang, C. Huan, D. Candela, R.W. Mair, R.L. Walsworth, Phys. Rev. Lett. 88 (2002) 44301.

[17] C. Huan, X. Yang, D. Candela, R.W. Mair, R.L. Walsworth, Phys. Rev. E 69 (2004) 41302.

[18] M. Nakagawa, S.A. Altobelli, A. Caprihan, E. Fukushima, E.-K. Jeong, Exp. Fluids 16 (1993) 54-60.

[19] K. Yamane, M. Nakagawa, S.A. Altobelli, T. Tanaka, Y. Tsuji, Phys. Fluids 10 (1998) 1419-1427.

[20] A. Caprihan, J.D. Seymour, J. Magn. Reson. 144 (2000) 96-107.

[21] G. Metcalf, M. Shattuck, Physica A 233 (1996) 709-717.

[22] M. Nakagawa, S.A. Altobelli, A. Caprihan, E. Fukushima, Chem. Engng Sci. 52 (1997) 4423-4428.

[23] K.M. Hill, A. Caprihan, J. Kakalios, Phys. Rev. Lett. 78 (1997) 50-53.

[24] K.M. Hill, A. Caprihan, J. Kakalios, Phys. Rev. E 56 (1997) 4386-4393.

[25] G. Metcalfe, L. Graham, J. Zhou, K. Liffman, Chaos 9 (1999) 581-593.

[26] A.V. Matveev, L.V. Barysheva, I.V. Koptyug, V.M. Khanaev, A.S. Noskov, Chem. Engng Sci. 61 (2006) 2394-2405.

[27] Blümich, NMR imaging of materials, Clarendon Press, Oxford, 2004.

[28] J.R. Moore, L. Garrido, J.L. Ackerman, Ceram. Engng Sci. Proc. 11 (1990) 1302-1319.

[29] M.S. Conradi, J. Magn. Reson. 93 (1991) 419-422.

[30] J.L. Ackerman, L. Garrido, J.R. Moore, B. Pfleiderer, Y. Wu, in: B. Blumich, W. Kuhn, (Eds.), Magnetic Resonance Microscopy. Methods and Applications in Materials Science, Agriculture and Biomedicine, VCH, Weinheim, 1992, pp. 237-260.

[31] I.V. Koptyug, D.R. Sagdeev, E. Gerkema, H. Van As, R.Z. Sagdeev, J. Magn. Reson. 175 (2005) 21-29.

[32] I.V. Koptyug, A.A. Lysova, R.Z. Sagdeev, V.A. Kirillov, A.V. Kulikov, V.N. Parmon, Catal. Today 105 (2005) 464-468.

[33] I.V. Koptyug, A.A. Lysova, in Stapf, S., Han, S. (Eds.), NMR Imaging in Chemical Engineering. Wiley-VCH, Weinheim, 2005, pp. 570-589.

[34] I.V. Koptyug, A.V. Khomichev, A.A. Lysova, R.Z. Sagdeev, Appl. Magn. Reson. 32 (2007), in press.

[35] I.V. Koptyug, A.A. Lysova, Bruker Spin Report, 157/158 (2006) 22-25.

[36] V. Antochshuk, M.-J. Kim, A.K. Khitrin, J. Magn. Reson. 167 (2004) 133-137.

[37] A. Abragam, The Principles of Nuclear Magnetism. Clarendon Press, Oxford, 1961.

Acknowledgments